Energy Proceedings
Vol 46, 2024
ISSN 2004-2965

Enhanced Gas Pipeline Multiple Leak Detection Using Artificial Neural Networks in Complex Multiphase Flow Conditions

Wahib A. Al-Ammari[1 *], Ahmad K. Sleiti[1]

1 Department of Mechanical & Industrial Engineering, College of Engineering, Qatar University, Doha, Qatar

* Corresponding Author: wahib.alammari@qu.edu.qa

ABSTRACT

When fast and accurate detection is crucial, such as in cases of pipeline leakage accidents, machine learning is a powerful tool for integrating real data with artificial intelligence. In this context, this study introduces reliable artificial neural network (ANN) models that are intended to precisely locate single or several leaks in undersea gas pipelines. Using OLGA multiphase software, thorough data for numerous leak scenarios are generated under multiphase flow conditions and based on an actual offshore pipeline profile. These data cover measurable flow variables (mass flow rate, temperature, and pressure) at the inlet and outlet of the monitored pipeline. The developed ANN models were trained to estimate the leak's location(s) and size(s) under single leak as well as multiple leak conditions, which have not been investigated before in open literature. The findings show that for single leak scenarios, the ANN models can detect and identify the leak size and location with an error of less than 1.0% across all phase flow scenarios. The leak localization error, however, is higher than 8.0% under multiple leak conditions. The outcomes of this study also show that the accuracy of the ANN models is significantly influenced by the phase flow conditions and number of ANN input parameters. To improve ANN performance and minimize the impact of noise signals, it is suggested to employ a multi-stage leak identification technique. To do this, an ANN model with two inputs must be utilized first, and subsequently, a model with six inputs must be progressively added. In this study, our approach and methods for generating leak-based data and identifying leaks in multiphase flow and various leak conditions can serve as a foundation for enhancing the efficiency and reliability of future machine learning-based leak detection systems.

Keywords: offshore gas pipelines; leak detection; leak localization; multiple leaks; multiphase flow; artificial neural network.

NONMENCLATURE

Abbreviations	
ANN	Artificial neural networks
CCA	Cross-correlation analysis
CPS-TLM	GPS- Time label method
CNN	convolutional neural network
HA	Harmonic analysis
GMM	Gaussian mixture models
LDA	Leak detection accuracy
LLA	Leak localization accuracy
LMD	Local mean decomposition
LSA	Leak size accuracy
NPW	Negative pressure wave
NNA	Neural network analysis
PPA	Pressure point analysis
RST	Rough set theory
SEM	State estimation method
SIM	System identification method
SRM	Supervised regression model
SVM	Support vector machine
TTBTs	Transient test-based techniques
V/MB	Volume/mass balance

1. INTRODUCTION

In 2020, natural gas supplied about 30% of the world's energy [1], [2], [3], reflecting the world's growing energy demand over the years. The natural gas pipeline system, which covers more than 2.2 million miles globally, is principally responsible for the transfer of natural gas products from the source to the end consumers [4]. However, with time, material flaws, abrasion, corrosion, and environmental variables harshly affected the pipeline networks, significantly reducing their integrity [5], which then resulted in leakage [6], [7]. The effects of gas pipeline leaks are significant, ranging from the incurrence of enormous costs to severe environmental degradation. Over the last thirty years,

This is a paper for 15th International Conference on Applied Energy (ICAE2023), Dec. 3-7, 2023, Doha, Qatar.

pipeline accidents in the United States alone have resulted in nearly $7 billion in damages [8] and numerous injuries. A notable incident occurred in late September to early October 2022 when substantial leaks of natural gas from the Nord Stream pipelines in the Baltic Sea near Denmark released approximately 220,000 tonnes of methane into the atmosphere [9], exacerbating global climate change. Therefore, it is urgently necessary to find efficient and practical ways to stop leaks in these pipeline networks.

Pipeline leak detection methods fall into two main categories: hardware-based and software-based techniques [10]. Hardware methods rely on physical sensors placed externally on the pipeline to detect escaping substances [11]. These sensors, including acoustic sensors [14], [15], fiber optic sensors [12], [13], and ground penetration radar [16], monitor changes in sound waves, pressure, or temperature that may indicate a leak. Fiber optic sensors utilize light to sense alterations in temperature and pressure [17], while acoustic sensors pick up sound waves produced by the escaping substance [18]. Ground penetration radar employs radio waves to detect changes in soil conductivity resulting from the escaping substance, aiding in leak localization [19].

Software methods employ algorithms and models [20] to monitor flow parameters, including PPA, NPA, and dynamic modeling [21]. PPA entails tracking pressure changes at different pipeline points to identify potential leaks [22]. NPW involves generating a pressure wave and measuring its travel time along the pipeline; deviations indicate leaks [23]. Dynamic modeling utilizes computer simulations to replicate pipeline flow conditions, offering high-precision leak detection and addressing data acquisition limitations. In-depth comparisons of these methods can be found in valuable review studies such as References [25], [26]. Table 1 provides a qualitative analysis of the performance indicators for software-based leak detection methods.

Dynamic modeling has traditionally been used to simulate and analyze hypothetical leak scenarios in oil and gas pipelines. However, it has limitations when it comes to real-time leak detection and demands substantial resources for execution. Consequently, machine learning has emerged as a more practical alternative. Machine learning employs algorithms that improve their performance through experience, allowing the development of mathematical models based on sample data. These models can swiftly and accurately predict or make decisions without the need for explicit programming. As a result, machine learning proves to be a valuable tool in connecting real data with artificial intelligence, particularly in critical areas like the rapid and precise detection of pipeline leaks [27].

Table 1. Qualitative analysis of the performance indicators of the various data-driven leak detection methods (Adapted from [28]).

Method	Adaptive ability	Localization accuracy	Response time	Sensitivity	Evaluation ability	False alarm rate	Maintenance	Cost
V/MB	×	▽	●	▽	▽	△	▼	▼
NPW	✓	▲	▲	●	▽	△	●	●
GPS-TLM	✓	▲	▲	●	▽	△	●	●
PPA	×	▽	●	●	▽	△	●	●
CCA	✓	●	▲	●	▽	●	●	●
TTBTs	✓	●	●	●	●	▼	△	●
SEM	✓	●	▽	●	●	△	△	△
SIM	✓	●	▽	●	●	△	△	△
NNA	✓	▽	▲	▲	▽	●	△	△
HA	✓	●	●	●	●	▼	△	●
Legend	✓= Can, × = Canot, ●= General, ▲= Good, Fast, Strong, ▼=Low, (advantage) △= High, ▽= Poor, Slow, Weak, (disadvantage)							

As indicated in Table 2, several research studies have utilized machine learning-based methods, including Gaussian mixture models, support vector machines (SVM), artificial neural networks (ANN), gradient boosting, decision trees, random forests, and deep learning techniques, for the purpose of detecting leaks in oil and gas pipelines. The majority of these studies have demonstrated remarkable precision in identifying, localizing, and categorizing leaks, achieving accuracy rates ranging from 90% to 99.4%. However, it is worth noting that while there is substantial research in the context of oil pipelines, there is a scarcity of machine learning-based studies focusing on leak detection in natural gas pipelines. Notably, Akinsete et al. [29], Xiao et al. [30], and Kim et al. [8] have investigated the detection of small leaks in gas pipelines using SVM and/or ANN-based models.

However, the data employed in their models was either single-phase flow-only or did not accurately reflect how the gas pipes actually operated. Additionally, the

connection between the input and outlet flow characteristics and the size and location of the leak were not examined. It is also important to note that there is no study that examines the performance of ANN-based models (or other machine learning techniques) under multiple leak conditions that is publicly available in the literature. The studies mentioned above only looked into one leak detection scenario.

Table 2. Accuracy of available leak detection studies in oil/gas pipelines using machine learning-based methods*.

Refs.	Method	Accuracy indicator
[8]	ANN	R^2=0.987.
[31]	ANN	90-95% (LDA)
[32]	ANN, Catboost	R^2=0.98 (Catboost)
[29]	ANN, SVM	R^2=0.998.
[33]	CNN	97% (LDA), 96% (LLA)
[30]	SVM	99.4% (LDA), 95.6% (LSA)
[34]	SVM+RST	95.17% (LDA)
[35]	SRM	CFD-based data, R^2=0.998
[36]	LMD + CasSVM	97.5% (LDA)

This paper proposes ANN models for precise leak detection and localization in offshore natural gas pipelines based on extensive data for single-, and multiphase flow conditions to fill the aforementioned shortcomings. This study also intended to determine how the ANN input settings affected the effectiveness of leak localization and detection. This study also examined pipeline flow and ANN-based models under various leak scenarios. The primary contributions of the current work can be summarized as follows:

a) Analyzing the leak detection parameters for single- and multiphase flow circumstances.
b) (b) Establishing systematic methods for generating data that can be utilized to build several data-driven models for leak detection.
c) (c) Evaluating the gas pipeline flow and examining how well the ANN-based leak identification model performs in various leak scenarios.

2. FLOWSHEET OF THE NEW LH2 PRODUCTION SYSTEM

The pipeline profile of an actual pipeline is used in the OLGA model of this study to create data for various leak sizes and locations which reflect actual field data. In the western offshore region of Myanmar, in the Bay of Bengal, this pipeline is in operation. The pipeline system, which has a 13 km length and a water depth range of 100 to 180 meters, is depicted in Fig. 1. Sensors placed at both ends of the pipe are used during the transit process to collect field data, such as flow rate, pressure, and temperature. As suggested in this study, the data gathered from these sensors can be utilized to examine flow behavior to identify leaks.

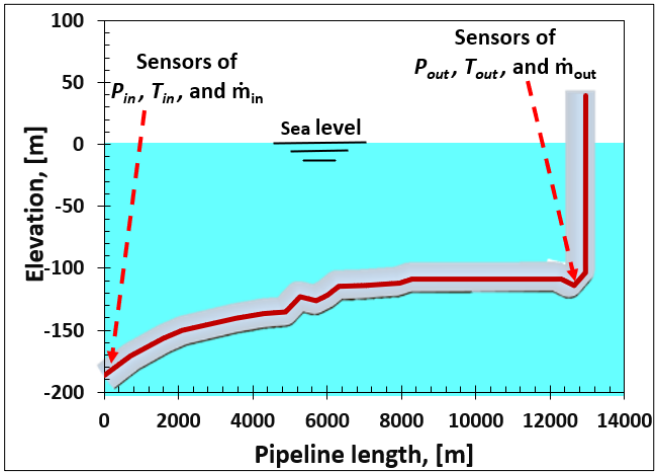

Fig. 1. OLGA pipeline profile (adapted from [8].

The material, dimensions, and boundary conditions of the pipeline must be established in order to simulate the flow behavior. Table 3 lists the key details of the pipeline geometry and flow characteristics.

Table 3. Design inputs for the pipeline model in OLGA.

Boundary Conditions	
Fluid	Natural Gas
Mass flow (kg/s)	65.0
Inlet temperature (°C)	53.0
Outlet temperature (°C)	27.0
Ambient temperature (°C)	12.
$U_{overall}$ (W/m^2-C)	200
Outlet pressure (bar)	83.0
Pipeline model specifications	
Material	Steel
Pipe thickness (mm)	9.0
Insulation thickness (mm)	20.0
Wall roughness (mm)	0.05
Pipe diameter (cm)	32.0
Pipe length (km)	13.0
# of sections	338
Section size (m)	50

3. METHODOLOGY

3.1 Data generation and validation

As depicted in Fig. 2, the PVT (pressure-volume-temperature [37]) file is first generated to be used in the OLGA-based pipeline model. This is done using an OLGA

Multiflash module to define the NG composition and its thermophysical properties. To precisely mimic the behavior of the gas in the pipeline, the PVT file comprises the thermodynamic parameters of the gas, including density, viscosity, and compressibility.

The pipeline geometry in OLGA was built using the pipeline profile depicted in Fig. 1. The pipeline's dimensions, layout, flow characteristics, and boundary conditions were entered into OLGA according to Table 3. 's specifications. The outcomes of the single-phase model are verified against actual field data, as will be explained below, before modeling the leak scenarios under multiphase situations. After that, since the ANN model requires a lot of data to be trained, the following comprehensive leak scenarios were set up and run: (1) The position of the leak was varied from 50 m to 12950 m with steps of 50 m, (2) At each leak location, the flow is simulated for a variety of leak sizes, ranging from 0.5 cm to 5 cm with steps of 0.5 cm, (3) For each phase flow, a total of 2590 data points were produced.

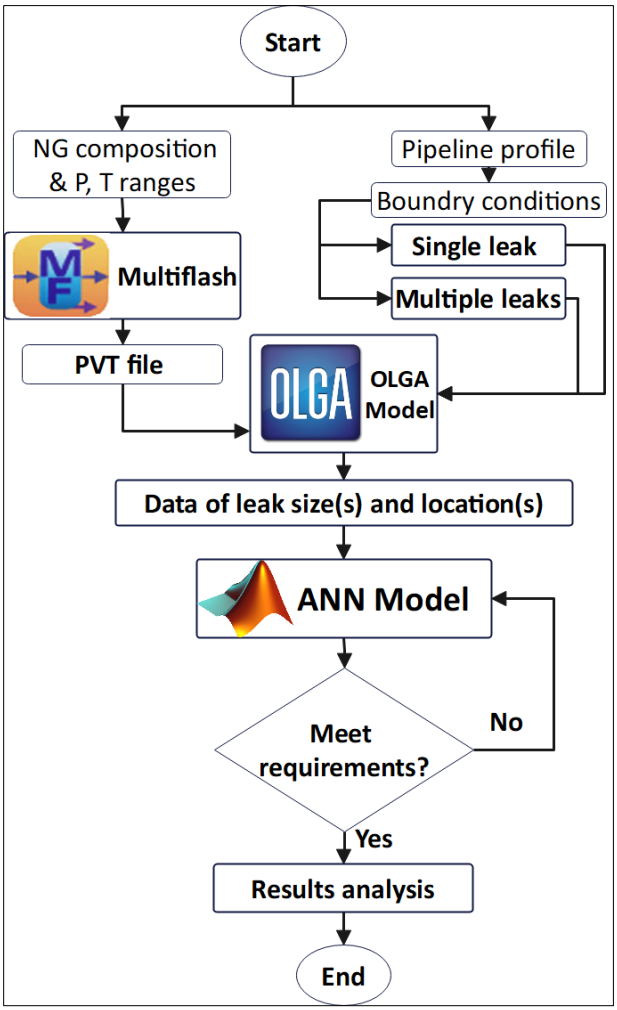

Fig. 2. Data generation, ANN training, and testing procedures.

After being normalized, the collected data are exported to MATLAB program where they are used to train, validate, and test the ANN model. The ANN-based data are then processed to Excel software for additional analysis if the model satisfies the error standards (for example, average relative error less than 1.0%). The model configuration is improved and altered until the error requirements are satisfied if the model fails to meet them.

In this work, the pressure profile derived by OLGA is compared with the real-field-based pressure profile as shown in Fig. 3 in order to validate the OLGA pipeline model. The real-field data used in this study's pipeline was sourced from [8]. Since there are no real-filed data for multiphase flow conditions, the validation process was done for single-phase flow conditions (with free leak). This comparison serves to validate the study's simulation strategy and methodology. The simulated pressure profile fits the real-filed profile with a relative error of less than 1%, as illustrated in Fig. 3.

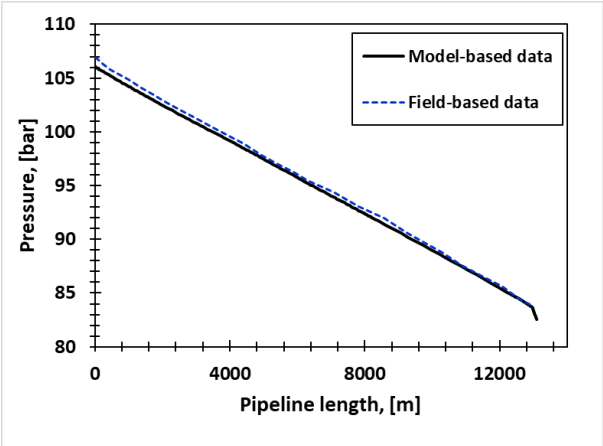

Fig. 3. Model pressure profile compared to real field data-based profile at “free” conditions.

The experimental data for a single leak and single-phase flow, available in [41], were also utilized to validate the accuracy of the OLGA model in predicting leak-based data. The experimental data were obtained from measurements conducted on a water pipeline with a total length of 1.6 m, an inner diameter of 12.7 mm, and an inlet flow rate of 0.32 kg/s. The measurements were taken under two conditions: "no leak" (with a leak percentage, LP, of 0%) and with a single leak positioned at x=0.73 m from the inlet of the pipe. As depicted in Fig. 4, the size of the leak was varied to obtain data for three different LPs (17%, 31%, and 50%). In OLGA software, the pipeline profile was created as a straight pipeline, and the boundary conditions were set to match the real experimental conditions. Subsequently, the pressure profiles data were generated in OLGA for both "no leak"

and single leak conditions and plotted alongside the experimental data for comparative analysis (see Fig. 4). It is noteworthy that the OLGA data exhibit a commendable agreement with the experimental data, displaying a maximum absolute error of less than 3.04%. This result underscores the capability of the OLGA model to generate leak-based data with sufficient accuracy for training artificial neural network (ANN) models.

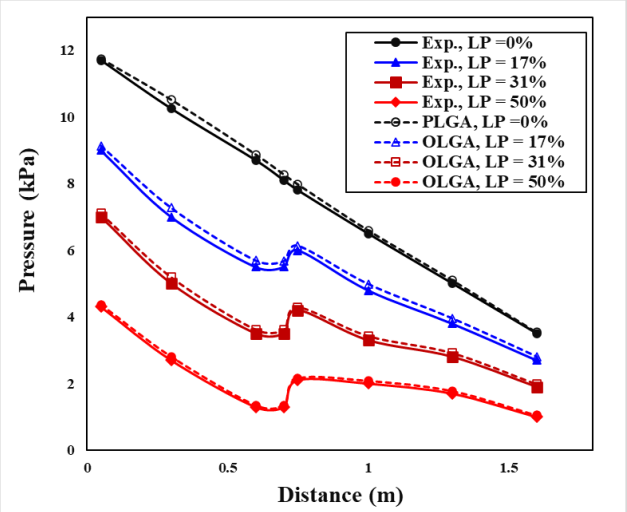

Fig. 4. Validation of OLGA model with experimental data under "no leak" and single leak conditions.

3.2 Machine learning model

For the ANN model for each phase flow in this study, a total of 2590 OLGA-based data points are utilized. Training data make up 70% of the data, followed by validation data (15%), and testing data (15%).

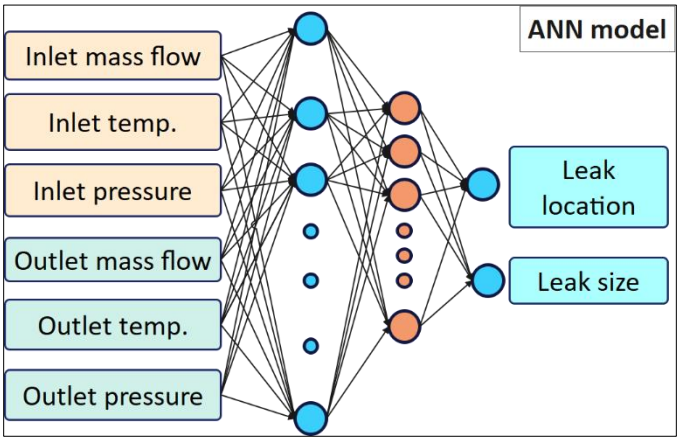

Fig. 5. ANN model Structure.

As illustrated in Fig. 5, the six input variables (six inputs group, SIG) employed for the neural network structure are the inlet and outlet temperature pressure, and flow rates. After that, utilizing the four-input group (FIG) and two-input group (TIG), the training, testing, and validation process is repeated. FIG includes outlet flow rate, outlet/inlet temperatures, and inlet pressure. Only the outlet mass flow, and inlet pressure are included in the TIG. These sets are created to look at how the ANN's input parameters affect the precision of leak detection and localization.

3.3 Data generation for multiple leaks analysis

The study involves evaluating the performance of an Artificial Neural Network (ANN)-based model for detecting leaks in pipelines. Initially, the model was analyzed for single leak detection in both single-phase and multiphase flow conditions. To extend its capabilities to multiple leak detection, the authors created a diverse dataset strategy. They divided the pipeline into sections consisting of ten joints each as shown in Fig. 6(a).

For single leak scenarios, data were generated at ten different locations along the pipeline, with three different leak sizes. This resulted in 30 datasets (Fig. 6(b)). For two leak scenarios, leak locations were systematically varied between joints, and leak sizes were adjusted, creating 45 sets of leak locations and nine groups of leak sizes, totaling 405 datasets (Fig. 6(c)). Similarly, for three leak scenarios, the researchers systematically adjusted leak locations and sizes, yielding 15 groups with 83 leak location sets each, totaling 1245 datasets (Fig. 6(d)). In total, 1680 datasets were generated, including data for input and output pressure, temperature, and mass flow. These datasets were then used to train and test the ANN model's performance in detecting multiple leaks.

4. RESULTS AND DISCUSSION

4.1 Single, two-, and multiphase flow analysis

This study examines the flow of natural gas in single- and two-phase flow scenarios in an offshore transmission pipeline. Three-phase flow refers to the flow of gas, water, and a trace amount of oil. Single-phase flow refers to the passage of gas alone. Two-phase flow refers to the flow of gas and liquid (often water). The fluctuations of the flow pressure, temperature, gas velocity, gas density, and gas flow across the pipeline length at the boundary conditions specified in Section 2 are simulated in the "free leak" scenario and shown in Fig. 7.

From Fig. 7, it is found that the gas velocity starts decreasing until about 4000 m and increases in the remaining length of the pipeline. This is basically explained by the nature of the actual pipeline profile as it starts with ramp direction then horizontal direction

after 6000 m. In addition, the temperature profile starts from the hot inlet temperature and decreases over the length of the pipeline due to the heat transfer process to the sea water. This yields a parabolic change in the gas density profiles which opposes the gas velocity and temperature behavior. This explains the linear decrease in the pipeline pressure.

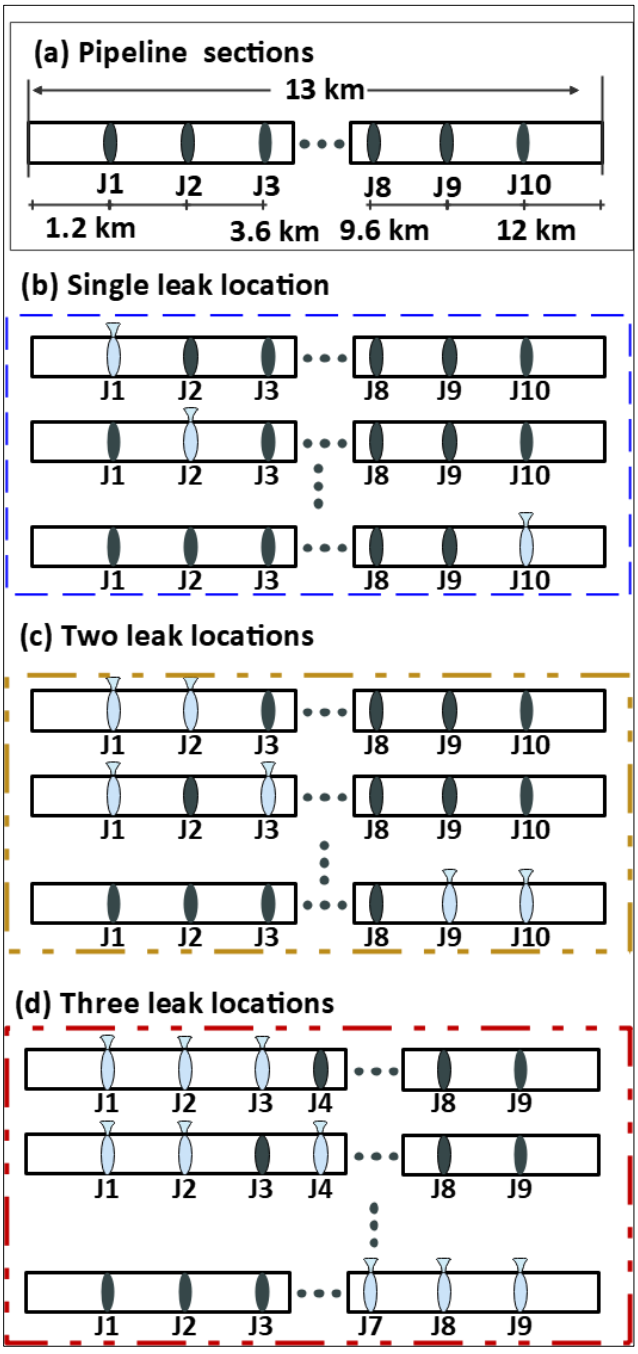

Fig. 6. Variation of leak location and number for multi-leak data generation.

The total mass flow rate curve shows constant flow under free leak conditions. This curve will be considered as a reference to compare the flow rate profile with "leak" conditions. Now, if we put a leak at any location of the pipeline, will this generate significant difference on the inlet/outlet flow parameters? To answer this, sample of the results under "single leak" conditions are presented in Fig. 8, Fig. 9 and Fig. 10.

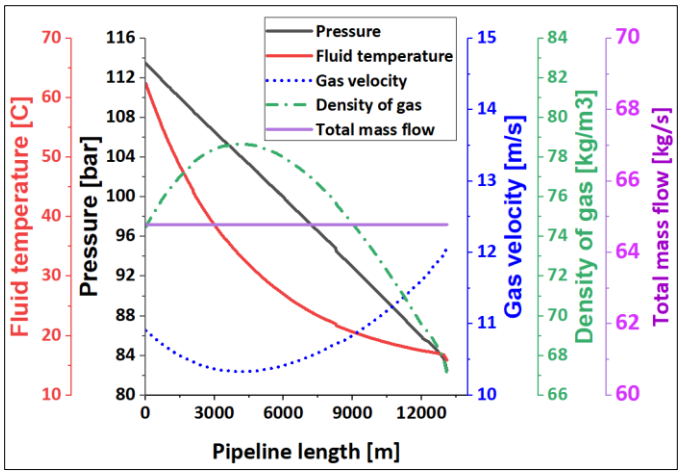

Fig. 7. Pressure, temperature, gas velocity, density, and mass flow rate over the pipeline length under "free leak" conditions (two-phase flow).

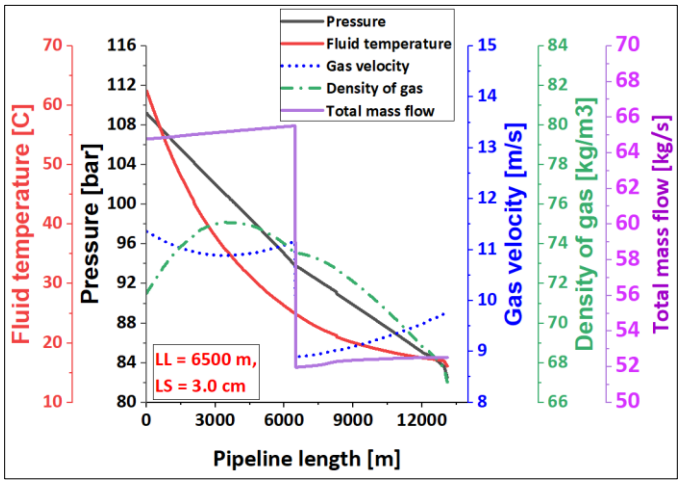

Fig. 8. Pressure profile for sample "leak" at 6500 m.

Fig. 8 shows the same parameters of Fig. 7 but with a single leak at 6500 m with leak size of 3.0 cm. it can be noted that the temperature profile is mostly the same as "free leak" profile. However, the inlet pressure is reduced from 114 bar (at "free leak") to 110 bar. Also, the outlet mass flow rate is reducing from the 65 kg/s to 53 kg/s. This reduction in the mass flow is noticeable due to the large size of the leak. However, for leaks with size lea than 0.50 cm, the reduction in the mass flow rate becomes very small (for single leak case).

In this context, we can note that the variation of the inlet pressure and outlet flow rate is more noticeable than of the change in the other parameters (inlet/outlet

temperatures). Therefore, these parameters are considered as basic input for the ANN models. However, the other inputs can be used as inputs to the ANN model to enhance its accuracy. However, using only two inputs will yield more robust results as the ANN will be less sensitive for noise signals.

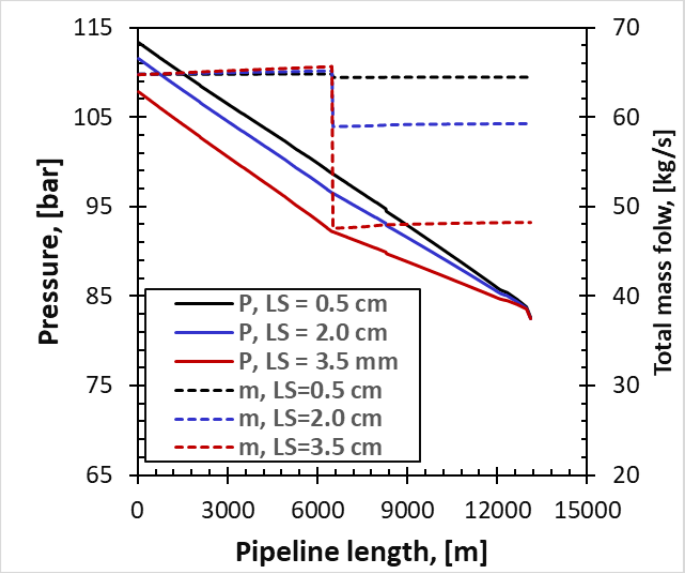

Fig. 9. Pressure and mass flow profiles for sample "leak" at 6500 m with three different leak sizes.

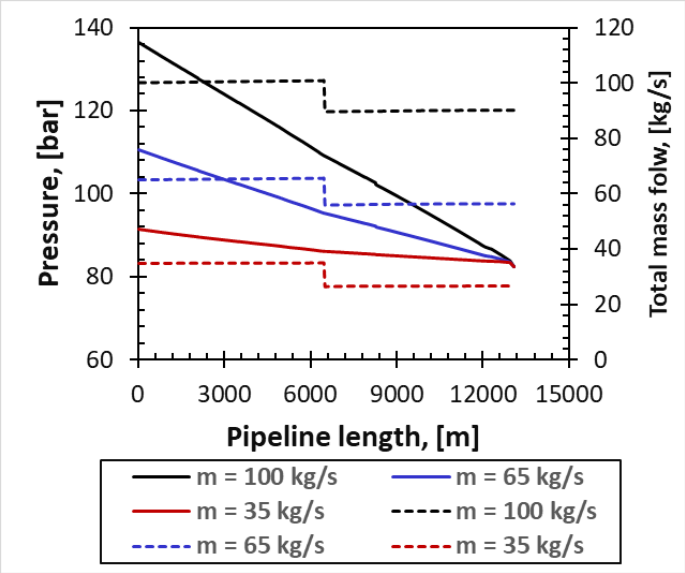

Fig. 10. Pressure and mass flow profiles for sample "leak" at 6500 m with three different mass flow rates.

Fig. 9 and Fig. 10 shows that different data set can be generated for different leak sizes, and different flow rates. Similarly, data can be generated for different pipeline diameters, outlet pressures, and other ambient conditions than those presented in the design condition discussed in Section 2. This is a necessary step to create comprehensive data for the ANN models. Based on these data, the ANN model will be able to detect leak size and locations under different operating conditions and transformable for different pipeline profiles and design conditions. Therefore, the ANN models were trained using comprehensive data generation strategy as discussed in Section 3.

4.2 Machine learning results

Table 4 displays the Absolute Relative Error (ARE) of an ANN model, averaged across three distinct data sets representing single-phase, two-phase, and three-phase flow conditions in offshore natural gas pipelines. The ANN model was trained and tested with varying numbers of input parameters (SIG, FIG, and TIG).

In the case of single-phase data, the ANN model achieved the lowest ARE for both leak size (0.1%) and leak location (0.6%) when trained and tested with six input parameters. When four input parameters were used, the ARE for leak size remained at 0.1%, but the accuracy for leak location slightly decreased to 1.4%. The model with only two input parameters exhibited the highest ARE values, with 0.9% for leak size and 4.8% for leak location, indicating a notable reduction in accuracy.

For two-phase data, the ANN model with four input parameters demonstrated the best performance with ARE values of 0.2% for leak size and 1.1% for leak location. Conversely, the model trained and tested with six input parameters had higher ARE values (0.6% for leak size and 2.3% for leak location). The model using only two input parameters had the lowest accuracy for leak size (0.3%) but the highest accuracy for leak location (1.3%).

4.3 Multiple leaks analysis

The simulated inlet and exit temperatures, pressures, and flow rates are generated for single, two, and three leak situations, with reference to the data generating procedure for multiple leaks illustrated in Section 3. The pressure and mass flow profiles are compared for a subset of cases prior to training the ANN model to make sure there are discernible differences between them. This stage is essential for the ANN model to effectively differentiate between the various scenarios based on the variances in the data that have been seen.

In three-phase data, the ANN model with only two input parameters exhibited the highest ARE values, with 1.2% for leak size and 4.8% for leak location. In summary, the results indicate that the model with six input parameters performs best for single-phase data, while

the model with four input parameters is optimal for two-phase data. For three-phase data, both the four-parameter and six-parameter models display competent performance in different aspects of leak detection and localization.

Table 4. ANN accuracy in terms of the Absolute relative error (ARE, %) *.

Flow phase	SIG		FIG		TIG	
	LS	LL	LS	LL	LS	LL
Single	0.1	0.6	0.1	1.4	0.9	4.8
Two	0.6	2.3	0.2	1.1	0.3	1.3
Three	0.3	3.4	0.5	4.8	1.2	4.8

*SIG, FIG, TIG= six, four, and two input group, respectively. LS = for leak size, LL = leak location.

For instance, Fig. 11 shows the flow parameters' profiles with three leaks at different locations and different sizes. This case is selected as example of that multiple leak case can yield input pressure and outlet flow rate similar to the values of single leak. To explain this, we can note that the inlet pressure in Fig. 11 is close to 109 bar with outlet flow close to 55 kg/s. These values close to those of single leak at 6500 m with size of 3.0 cm (110 bar, 53 kg/s). This may yield inaccurate prediction for the leak detection and localization if the ANN model is not supported with other inputs. Therefore, for multiple leak detection, it will be more effective to start leak detection with two ANN inputs (inlet pressure, and outlet mass flow rate). Then, to verify the results, re-detect with four inputs and six inputs to the ANN models. This will enhance the accuracy of the ANN model as explained in the next subsections.

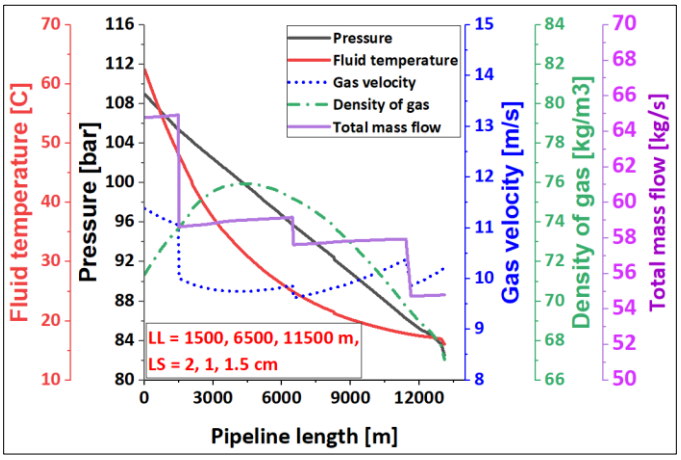

Fig. 11. Pressure, temperature, gas velocity, density, and mass flow profiles with three leak locations.

To begin predicting leak sizes and locations, it's essential to first determine the total number of leaks. To achieve this, a pattern recognition ANN model is employed, exhibiting a flawless 100% accuracy rate. Once the number of leaks is established, the feedforward ANN model is utilized to predict leak locations and sizes. Table 5 offers a comparative overview of the ANN model's performance in single, two, and three leak scenarios, providing insights into the optimal ANN configurations and Absolute Relative Error (ARE) values for leak size and location predictions.

For the single leak scenario, the preferred ANN configuration is a single hidden layer comprising ten neurons, denoted as "10." The ARE values for leak size and location are 1.80% and 2.76%, respectively. It's worth noting that these values are notably higher than those reported in Table 4 for the single leak scenario (0.6% for leak size and 2.3% for leak location). The discrepancy can be attributed to differences in the number of data sets used for training and testing the ANN model.

Table 5. Accuracy measures of the ANN models for single/ two/three leaks' conditions *.

# of leaks	ANN config.	ARE (leak size)	ARE (leak location)
Single	"10"	1.80	2.76
Two	"15,2"	9.18	16.18
Three	"16,20"	8.58	10.59

*ARE= $\frac{1}{n} \times \sum_{i=1}^{i=n} \left(\frac{|Predicted\ value - actual\ value|}{actual\ value}\right)$

In the two leaks scenario, the optimal ANN configuration is denoted as "15,25." However, the ARE values are higher compared to the single leak scenario, with a 9.18% average relative error for leak size and a 16.18% average relative error for leak location.

In the three leaks scenario, the optimal ANN configuration is labeled "16, 20." Again, the ARE values are higher than those in the single leak scenario, with an 8.58% average relative error for leak size and a 10.59% average relative error for leak location.

In summary, the analysis of ARE values reveals that the ANN model excels in the single leak scenario, displaying high accuracy in both leak size and location predictions. However, its performance is poor in scenarios with two or three leaks, as evidenced by the higher ARE values. This implies that accurately predicting both the size and location of multiple leaks presents challenges for the ANN model, resulting in increased

uncertainty and errors in such cases. Further investigation and assessment are needed to identify potential factors contributing to the performance decline in multiple leak scenarios and explore strategies to enhance the ANN model's accuracy in such situations.

5. CONCLUSIONS

This paper introduces new methodologies to develop efficient artificial neural network (ANN) models for leak detection and localization in offshore gas pipelines. Systematic procedures are developed to generate data under single/multiple leak conditions to train and test ANN-based leak detection and localization models. These data are generated based on real pipeline profile and cover single-, two-, and three phase flow conditions (using OLGA multiphase simulator).

First, the pipeline's input and output pressure, temperature, and mass flow rates were used to train the ANN models. These six input variables are referred to as the SIG (six inputs group). The ANN's input count is then changed to four (FIG), and two (TIG) inputs. The findings demonstrate that the projected values of the leak size and leak position are significantly influenced by the number of ANN inputs (SIG, FIG, and TIG) as well as the phase flow conditions. Therefore, a multi-stage leak identification procedure starting with TIG and confirming it using FIG and SIG ANN models is suggested in order to obtain robust leak determination parameters and minimize noise signals.

For multiple leak scenarios, data are generated based on two-phase flow conditions and single, two, and three leaks' locations. The results show that the accuracy of the ANN models at multiple leak conditions is much lower than at single leak with an average error higher than 8%. Therefore, to improve the multiple leak detection accuracy, more data need to generated and further tests for these data with various machine learning techniques are required and recommended as a future work.

ACKNOWLEDGEMENT

The work presented in this publication was made possible by NPRP-S grant # [NPRP14S-0321-210080] from the Qatar National Research Fund (a member of Qatar Foundation). The findings herein reflect the work, and are solely the responsibility, of the authors.

REFERENCE

[1] S. (Acting E. A. Nalley and A. (Assistant A. for E. A. LaRose, "Highlights, Annual Energy Outlook," vol. 2022, 2022.

[2] A. K. Sleiti and W. A. Al-Ammari, "Novel integration between propane pre-cooled mixed refrigerant LNG process and concentrated solar power system based on supercritical CO2 power cycle," Energy Reports, vol. Under Revi, 2022.

[3] A. K. Sleiti, W. A. Al-Ammari, and K. M. Aboueata, "Flare gas-to-power by direct intercooled oxy-combustion supercritical CO2 power cycles," Fuel, vol. 308, no. August 2021, p. 121808, 2022, doi: 10.1016/j.fuel.2021.121808.

[4] S. Kumar Vandrangi, T. Alemu Lemma, S. Muhammad Mujtaba, and T. N. Ofei, "Developments of leak detection, diagnostics, and prediction algorithms in multiphase flows," Chem. Eng. Sci., vol. 248, p. 117205, 2022, doi: 10.1016/j.ces.2021.117205.

[5] Ahmad K. Sleiti, W. A. Al-Ammari, L. Vesely, and J. S. Kapat, "Carbon Dioxide Transport Pipeline Systems: Overview of Technical Characteristics, Safety, Integrity and Cost, and Potential Application of Digital Twin," J. Energy Resour. Technol., vol. 144, no. 9, p. 092106, 2022, doi: https://doi.org/10.1115/1.4053348.

[6] H. Wang and I. J. Duncan, "Likelihood, causes, and consequences of focused leakage and rupture of U.S. natural gas transmission pipelines," J. Loss Prev. Process Ind., vol. 30, no. 1, pp. 177–187, 2014, doi: 10.1016/j.jlp.2014.05.009.

[7] I. Bolotina, V. Borikov, V. Ivanova, K. Mertins, and S. Uchaikin, "Application of phased antenna arrays for pipeline leak detection," J. Pet. Sci. Eng., vol. 161, no. June 2017, pp. 497–505, 2018, doi: 10.1016/j.petrol.2017.10.059.

[8] J. Kim, M. Chae, J. Han, S. Park, and Y. Lee, "The development of leak detection model in subsea gas pipeline using machine learning," J. Nat. Gas Sci. Eng., vol. 94, no. July, p. 104134, 2021, doi: 10.1016/j.jngse.2021.104134.

[9] M. Jia et al., "The Nord Stream pipeline gas leaks released approximately 220,000 tonnes of methane into the atmosphere," Environ. Sci. Ecotechnology, vol. 12, p. 100210, 2022, doi: 10.1016/j.ese.2022.100210.

[10] N. V. S. Korlapati, F. Khan, Q. Noor, S. Mirza, and S. Vaddiraju, "Review and analysis of pipeline leak detection methods," J. Pipeline Sci. Eng., vol. 2, no. 4, p. 100074, 2022, doi: 10.1016/j.jpse.2022.100074.

[11] G. Geiger, "State-of-the-art in leak detection and localization," Erdoel Erdgas Kohle, vol. 122, no. 12, pp. 193–198, 2006.

[12] M. Nikles et al., "Leakage detection using fiber optics distributed temperature monitoring," Smart Struct. Mater. 2004 Smart Sens. Technol. Meas. Syst., vol. 5384, p. 18, 2004, doi: 10.1117/12.540270.

[13] B. Vogel, C. Cassens, A. Graupner, and A. Trostel, “Leakage detection systems by using distributed fiber optical temperature measurement,” Smart Struct. Mater. 2001 Sens. Phenom. Meas. Instrum. Smart Struct. Mater., vol. 4328, p. 23, 2001, doi: 10.1117/12.435546.
[14] C. W. Liu, Y. X. Li, Y. K. Yan, J. T. Fu, and Y. Q. Zhang, “A new leak location method based on leakage acoustic waves for oil and gas pipelines,” J. Loss Prev. Process Ind., vol. 35, pp. 236–246, 2015, doi: 10.1016/j.jlp.2015.05.006.
[15] C. Liu, Y. Li, L. Fang, and M. Xu, “Experimental study on a de-noising system for gas and oil pipelines based on an acoustic leak detection and location method,” Int. J. Press. Vessel. Pip., vol. 151, pp. 20–34, 2017, doi: 10.1016/j.ijpvp.2017.02.001.
[16] J. J. Daniels, R. Roberts, and M. Vendl, “Ground penetrating radar for the detection of liquid contaminants,” J. Appl. Geophys., vol. 33, no. 1–3, pp. 195–207, 1995, doi: 10.1016/0926-9851(95)90041-1.
[17] A. Myles, “Permanent Leak Detection on Pipes Using a Fibre Optic Based Continuous Sensor Technology,” Pipelines 2011 A Sound Conduit Shar. Solut. - Proc. Pipelines 2011 Conf., pp. 744–754, 2011, doi: 10.1061/41187(420)69.
[18] A. B. Lukonge and X. Cao, “Leak Detection System for Long-Distance Onshore and Offshore Gas Pipeline Using Acoustic Emission Technology. A Review,” Trans. Indian Inst. Met., vol. 73, no. 7, pp. 1715–1727, 2020, doi: 10.1007/s12666-020-02002-x.
[19] M. Lawrence, K. B. Sc, C. Eng, and G. P. R. G. Services, “Locating a subsurface oil leak using ground penetrating radar,” vol. 4084, 2000.
[20] K. G. Aljuaid, M. A. Albuoderman, E. A. Alahmadi, and J. Iqbal, “Comparative review of pipelines monitoring and leakage detection techniques,” 2020 2nd Int. Conf. Comput. Inf. Sci. ICCIS 2020, 2020, doi: 10.1109/ICCIS49240.2020.9257602.
[21] E. Hauge, O. M. Aamo, and J. M. Godhavn, “Model-based monitoring and leak detection in oil and gas pipelines,” SPE Proj. Facil. Constr., vol. 4, no. 3, pp. 53–60, 2009, doi: 10.2118/114218-PA.
[22] A. B. M. Akib, N. Bin Saad, and V. Asirvadam, “Pressure point analysis for early detection system,” Proc. - 2011 IEEE 7th Int. Colloq. Signal Process. Its Appl. CSPA 2011, pp. 103–107, 2011, doi: 10.1109/CSPA.2011.5759852.
[23] C. H. Tian, J. C. Yan, J. Huang, Y. Wang, D. S. Kim, and T. Yi, “Negative pressure wave based pipeline Leak Detection: Challenges and algorithms,” Proc. 2012 IEEE Int. Conf. Serv. Oper. Logist. Informatics, SOLI 2012, pp. 372–376, 2012, doi: 10.1109/SOLI.2012.6273565.
[24] S. K. Vandrangi, T. A. Lemma, S. M. Mujtaba, and S. R. Pedapati, “Determination and analysis of leak estimation parameters in two-phase flow pipelines using OLGA multiphase software,” Sustain. Comput. Informatics Syst., vol. 31, no. February, p. 100564, 2021, doi: 10.1016/j.suscom.2021.100564.
[25] N. Behari, M. Z. Sheriff, M. A. Rahman, M. Nounou, I. Hassan, and H. Nounou, “Chronic leak detection for single and multiphase flow: A critical review on onshore and offshore subsea and arctic conditions,” J. Nat. Gas Sci. Eng., vol. 81, no. January, p. 103460, 2020, doi: 10.1016/j.jngse.2020.103460.
[26] D. Zaman, M. K. Tiwari, A. K. Gupta, and D. Sen, “A review of leakage detection strategies for pressurised pipeline in steady-state,” Eng. Fail. Anal., vol. 109, no. November 2019, p. 104264, 2020, doi: 10.1016/j.engfailanal.2019.104264.
[27] Y. AbuShanab, W. A. Al-Ammari, S. Gowid, and A. K. Sleiti, “Accurate prediction of dynamic viscosity of polyalpha-olefin boron nitride nanofluids using machine learning,” Heliyon, vol. 9, no. 6, 2023, doi: 10.1016/j.heliyon.2023.e16716.
[28] H. Lu, T. Iseley, S. Behbahani, and L. Fu, “Leakage detection techniques for oil and gas pipelines: State-of-the-art,” Tunn. Undergr. Sp. Technol., vol. 98, no. November 2018, 2020, doi: 10.1016/j.tust.2019.103249.
[29] O. Akinsete and A. Oshingbesan, “Leak detection in natural gas pipelines using intelligent models,” 2019. doi: 10.2118/198738-MS.
[30] R. Xiao, Q. Hu, and J. Li, “Leak detection of gas pipelines using acoustic signals based on wavelet transform and Support Vector Machine,” Measurement, vol. 146, pp. 479–489, Nov. 2019, doi: 10.1016/J.MEASUREMENT.2019.06.050.
[31] P. Kumari, S. Z. Halim, J. S. Il Kwon, and N. Quddus, “An integrated risk prediction model for corrosion-induced pipeline incidents using artificial neural network and Bayesian analysis,” Process Saf. Environ. Prot., vol. 167, no. July, pp. 34–44, 2022, doi: 10.1016/j.psep.2022.07.053.
[32] W. Liu;, Z. Chen;, and Y. Hu, “Failure Pressure Prediction of Defective Pipeline Using Finite Element Method and Machine Learning Models,” in SPE Annual Technical Conference and Exhibition, 2022, p. SPE-210406-MS. doi: https://doi.org/10.2118/210406-MS.
[33] J. Yang, H. Mostaghimi, R. Hugo, and S. S. Park, “Pipeline leak and volume rate detections through Artificial intelligence and vibration analysis,” Measurement, vol. 187, p. 110368, Jan. 2022, doi: 10.1016/J.MEASUREMENT.2021.110368.

[34] S. K. Mandal, F. T. S. Chan, and M. K. Tiwari, “Leak detection of pipeline: An integrated approach of rough set theory and artificial bee colony trained SVM,” Expert Syst. Appl., vol. 39, no. 3, pp. 3071–3080, Feb. 2012, doi: 10.1016/J.ESWA.2011.08.170.
[35] D. Eastvedt, G. Naterer, and X. Duan, “Detection of faults in subsea pipelines by flow monitoring with regression supervised machine learning,” Process Saf. Environ. Prot., vol. 161, pp. 409–420, 2022, doi: 10.1016/j.psep.2022.03.049.
[36] M. Zhou, Q. Zhang, Y. Liu, X. Sun, Y. Cai, and H. Pan, “An Integration Method Using Kernel Principal Component Analysis and Cascade Support Vector Data Description for Pipeline Leak Detection with Multiple Operating Modes,” Processes, vol. 7, no. 10, p. 648, 2019.
[37] A. K. Sleiti et al., “Comprehensive assessment and evaluation of correlations for gas-oil ratio, oil formation volume factor, gas viscosity, and gas density utilized in gas kick detection,” J. Pet. Sci. Eng., vol. 207, no. May, p. 109135, 2021, doi: 10.1016/j.petrol.2021.109135.